

Helical Structures of *Z,Z*-1,4-Bis(3,5-di-*tert*-butylstyryl)benzene and *Z,Z,Z*-4,4'-Bis(3,5-di-*tert*-butylstyryl)stilbene in the Solid State

Mikael Håkansson,^a Susan Jagner,^a Mikael Sundahl^b and Olof Wennerström^{b,*}

^aDepartment of Inorganic Chemistry and ^bDepartment of Organic Chemistry, Chalmers University of Technology, S-412 96 Göteborg, Sweden

Håkansson, M., Jagner, S., Sundahl, M. and Wennerström, O., 1992. Helical Structures of *Z,Z*-1,4-Bis(3,5-di-*tert*-butylstyryl)benzene and *Z,Z,Z*-4,4'-Bis(3,5-di-*tert*-butylstyryl)stilbene in the Solid State. – Acta Chem. Scand. 46: 1160–1165.

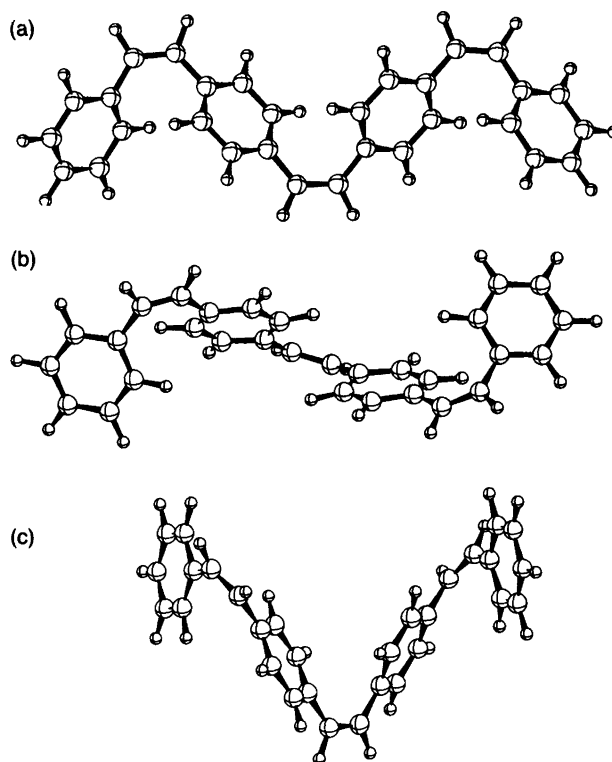
The crystal structures of the two title compounds, a bis(styryl)benzene and a bis(styryl)stilbene, containing three and four benzene rings, respectively, joined by vinylene groups, show that both have open helical structures which still permit some π -electron overlap along the conjugated chains. The π -electron conjugation and its relevance to the photochemical behavior of the compounds is discussed.

Z- and *E*-Stilbene are basic reference compounds for photochemical isomerizations and photocyclizations.¹ For a recent study of the *Z/E* photoisomerization of stilbenes with styrylsubstituents in the 4- (and 4'-)position(s) we have prepared all three configurational isomers of 1,4-bis(3,5-di-*tert*-butylstyryl)benzene² and all six isomers of 4,4'-bis(3,5-di-*tert*-butylstyryl)stilbene. The *tert*-butyl groups were introduced into the *meta* positions in two of the phenyl rings to increase the solubility of the compounds. The different isomers in the two series can readily be separated by HPLC methods and their structures determined by ¹H NMR and UV spectra and mass spectrometry. To avoid any uncertainty about the structure of the configurational isomers, and, more importantly, to acquire knowledge about their preferred conformations and the structure of their π -systems, we have carried out an X-ray structure determination of one isomer from each series with the double bonds in the *Z* (*cis*) configurations, i.e. the title compounds *Z,Z*-1,4-bis(3,5-di-*tert*-butylstyryl)benzene, **1**, and *Z,Z,Z*-4,4'-bis(3,5-di-*tert*-butylstyryl)stilbene, **2**.

The compounds can exist in several different conformations of similar energy in solution, some of which are shown in Scheme 1 for the 4,4'-bis(3,5-di-*tert*-butylstyryl)stilbene series. A similar series of conformers also exist for the 1,4-bis(3,5-di-*tert*-butylstyryl)benzenes.

If a straight-chain orientation of the benzene rings is preferred, these then have to be tilted to reduce the steric interaction between the *ortho*-hydrogens. Two general structures are possible. If the chain extends from different sides of the inner benzene rings then a regular chain as depicted as (a) in Scheme 1 is generated. If the chains extend from the same side of the inner benzene rings then a helical structure with a narrow diameter is generated (b) in

Scheme 1. Alternatively, a more open helical orientation of the benzene rings as shown in (c) in Scheme 1 might be the preferred one. The latter structure is quite interesting, with a relatively large diameter and still a significant overlap of the π -system along the axis of the helix. Molecular-mechanics calculations cannot differentiate unambiguously between the possible conformations, since they have very similar energies. The same could also be true for advanced



Scheme 1. Three regular conformers of similar energy of *Z,Z,Z*-4,4'-bis(styryl)stilbene: (a) chain, (b) extended helix and (c) helix.

* To whom correspondence should be addressed.

Table 1. Crystal and experimental data for C₃₈H₅₀ (1) and C₄₆H₅₆ · 0.25CH₂Cl₂ · 0.5H₂O (2).

	1	2
<i>M_r</i>	506.8	637.7
Unit cell dimensions		
<i>a</i> /Å	9.665(5)	14.789(5)
<i>b</i> /Å	22.315(4)	—
<i>c</i> /Å	15.298(4)	17.995(10)
β/°	97.76(3)	—
<i>V</i> /Å ³	3269(3)	3936(3)
Space group	<i>P</i> 2 ₁ / <i>n</i>	<i>P</i> 4 ₂ / <i>n</i>
<i>Z</i>	4	4
<i>D_c</i> /g cm ⁻³	1.03	1.08
Habit	Colourless prisms	Colourless tetragonal prisms
Crystal size/mm	0.40 × 0.30 × 0.30	0.40 × 0.40 × 0.30
μ(MoKα)/cm ⁻¹	0.53	0.90
Abs. correction	None	None
<i>F</i> (000)	1112	1384
Refls. measured	+ <i>h</i> , + <i>k</i> , ± <i>l</i>	+ <i>h</i> , + <i>k</i> , + <i>l</i>
<i>T</i> /K	133	296
2θ range/°	3.5 < 2θ < 45	3.5 < 2θ < 50
2θ scan rate/° min ⁻¹	16	2
Scan width/°	(1.15 + 0.30 tan θ)	(1.37 + 0.30 tan θ)
No. unique refls.	4395	3602
No. obs. refls.	2494	1431
No. par. refined	343	221
<i>R</i>	0.071	0.082
<i>R_w</i>	0.093	0.085
Max. min. residual electron density/e Å ⁻³	1.02; -0.35	0.41; -0.37

quantum-mechanical calculations. An X-ray structure ought, however, to solve this problem and reveal which conformer is preferred in the solid state.

It is also of interest to evaluate the twist angle between the vinylene bridges and the benzene rings, and thus the extent of π-electron overlap along the conjugated system, since the *Z/E* photoisomerization of these compounds occurs by a different mechanism from that of stilbene itself. In stilbene, non-adiabatic photoisomerizations are the dominant reactions,¹ whereas adiabatic processes can occur on irradiation of the two parent compounds under proper conditions. This is caused by relatively small changes of the energy difference between the planar and twisted conformations on the first excited singlet and triplet surfaces. A deeper understanding of this change in mechanism for the photoisomerization will require extensive calculations which should be based on correct structural information.

Synthesis

The synthesis of **1** has been reported earlier.² Compound **2** was prepared by a similar method, a Wittig reaction between 4,4'-*cis*-stilbenedialdehyde and the phosphonium salt from 3,5-*tert*-butylbenzylbromide and triphenylphosphine. Wittig reactions with semi-stabilized ylides always yield mixtures of *Z* and *E* isomers.³ Thus in the synthesis of **2**, three isomers are formed. The isomers were separated by preparative HPLC; for experimental details see Ref. 2.

Z,Z,Z-Isomer, 43 %, m.p. 83–88 °C; *Z,Z,E*-isomer, 30 %, m.p. 119–124 °C; *E,Z,E*-isomer, 15 %, m.p. 166–170 °C. The *Z,Z,Z*-isomer, used for the crystallography, was recrystallized from an ethanol–water–CH₂Cl₂ mixture (85:10:5). The isomers can also be recrystallized from 95:5 ethanol–water.

Z,Z,Z isomer. ¹H NMR (400 MHz, CDCl₃) δ 7.22 (t, *J* = 2 Hz, 2H), 7.14 (d, *J* = 9 Hz, 4H), 7.14 (d, *J* = 9 Hz, 4H), 7.13 (d, *J* = 2 Hz, 4H), 6.57 (d, *J* = 12 Hz, 2H), 6.50 (s, 2H), 6.49 (d, *J* = 12 Hz, 1H), 1.21 (s, 36H). UV (cyclohexane): λ_{max} 331.5 (ε = 20 200), 300 (20 800).

Z,Z,E isomer. ¹H NMR (400 MHz, CDCl₃) δ 7.38 (d, *J* = 8 Hz, 2H), 7.35 (s, 2H), 7.27 (d, *J* = 8 Hz, 2H), 7.26 (s, 1H), 7.24 (t, *J* = 2 Hz, 1H), 7.17 (d, *J* = 8 Hz, 2H), 7.16 (d, *J* = 8 Hz, 2H), 7.15 (d, *J* = 2 Hz, 2H), 7.12 (d, *J* = 16 Hz, 1H), 7.03 (d, *J* = 16 Hz, 1H), 6.59 (d, *J* = 12 Hz, 1H), 6.55 (d, *J* = 12 Hz, 1H), 6.53 (d, *J* = 12 Hz, 1H), 6.50 (d, *J* = 12 Hz, 1H), 1.36 (s, 18H), 1.25 (s, 18H). UV (cyclohexane): λ_{max} 331.5 (ε = 35 300), 306 (34 200).

E,Z,E isomer. ¹H NMR (400 MHz, CDCl₃) δ 7.41 (d, *J* = 8 Hz, 4H), 7.35 (s, 6H), 7.30 (d, *J* = 8 Hz, 4H), 7.14 (d, *J* = 16 Hz, 2H), 7.05 (d, *J* = 16 Hz, 2H), 6.58 (s, 2H), 1.36 (s, 36H). UV (cyclohexane): λ_{max} 353 (ε = 41 900), 316 (50 700).

Crystallography

Crystal and experimental data for C₃₈H₅₀ (**1**) and C₄₆H₅₆ · 0.25CH₂Cl₂ · 0.5H₂O (**2**) are given in Table 1. Diffracted intensities were measured with a Rigaku AF6CR diffractometer using graphite-monochromated MoKα radiation (λ = 0.7107 Å) from an RU200 rotating anode source operated at 9 kW (50 kV; 180 mA). Weak reflections [*I* < 10σ(*I*)] were rescanned up to three times and counts accumulated to improve counting statistics. Stationary background counts were recorded on each side of the reflection, the ratio of peak counting time vs. background counting time being 2:1. Three reflections monitored at regular intervals (after every 150 reflections measured) showed no evidence of crystal decay in either case. Intensities were corrected for Lorentz and polarisation effects, but no corrections were made for the effects of absorption. Cell constants were determined from the setting angles of 25 reflections in the range 38.4 < 2θ < 44.4 (**1**) and 22.5 < 2θ < 36.8° (**2**). Reflections for which *I* > 3.0σ(*I*) were regarded as being observed. The structures were solved by direct methods (MITHRIL)⁴ and subsequent electron-density calculations, and refined by full-matrix least-squares methods. In **1**, anisotropic thermal parameters were refined for the non-hydrogen atoms, and the hydrogen atoms were included as a fixed contribution in calculated positions (C–H = 0.95 Å; *B* = 1.2 × *B*_{eq}*)

$$* B_{eq} = \frac{8\pi^2}{3} \sum_i \sum_j U_{ij} a_i^* a_j^* a_i \cdot a_j$$

Table 2. Positional and equivalent isotropic thermal parameters, B_{eq} (in Å²), for the non-hydrogen atoms in $\text{C}_{38}\text{H}_{50}$ (**1**).

Atom	x	y	z	B_{eq}
C(1)	1.014(1)	0.0742(4)	0.6288(7)	10.7(6)
C(2)	1.050(1)	0.1239(6)	0.4909(7)	14.1(8)
C(3)	1.122(1)	0.1660(6)	0.621(1)	15(1)
C(4)	0.9992(6)	0.1248(3)	0.5733(4)	4.6(3)
C(5)	0.8646(6)	0.1599(3)	0.5774(4)	3.1(3)
C(6)	0.8218(6)	0.1748(3)	0.6576(4)	3.0(3)
C(7)	0.7007(5)	0.2070(2)	0.6631(3)	2.3(2)
C(8)	0.6164(5)	0.2225(2)	0.5847(4)	2.4(2)
C(9)	0.6513(5)	0.2077(2)	0.5026(3)	2.4(2)
C(10)	0.7777(6)	0.1764(2)	0.5004(4)	3.0(3)
C(11)	0.5494(5)	0.2225(2)	0.4204(3)	2.7(2)
C(12)	0.6078(7)	0.2080(3)	0.3348(4)	4.5(3)
C(13)	0.4171(7)	0.1848(3)	0.4241(4)	4.7(3)
C(14)	0.5108(6)	0.2883(3)	0.4192(4)	3.7(3)
C(15)	0.6554(6)	0.2189(3)	0.7499(3)	2.9(3)
C(16)	0.5917(6)	0.2671(3)	0.7766(3)	3.0(3)
C(17)	0.5585(5)	0.3252(2)	0.7321(3)	2.7(3)
C(18)	0.4392(6)	0.3565(3)	0.7486(4)	3.7(3)
C(19)	0.4066(6)	0.4113(3)	0.7107(4)	3.6(3)
C(20)	0.4921(5)	0.4400(2)	0.6583(3)	2.5(2)
C(21)	0.6116(5)	0.4091(2)	0.6417(3)	2.6(3)
C(22)	0.6440(5)	0.3535(2)	0.6780(4)	2.6(2)
C(23)	0.4502(5)	0.4984(3)	0.6197(3)	2.6(3)
C(24)	0.5279(5)	0.5447(3)	0.6005(3)	2.7(3)
C(25)	0.6802(5)	0.5528(2)	0.6223(3)	2.1(2)
C(26)	0.7544(6)	0.5823(2)	0.5633(3)	2.6(3)
C(27)	0.8983(6)	0.5914(2)	0.5822(4)	2.5(3)
C(28)	0.9649(5)	0.5712(2)	0.6632(4)	2.5(2)
C(29)	0.8942(5)	0.5424(2)	0.7249(3)	2.2(2)
C(30)	0.7508(5)	0.5336(2)	0.7027(3)	2.5(2)
C(31)	0.9725(4)	0.5218(2)	0.8134(3)	2.6(2)
C(32)	0.8795(7)	0.4884(4)	0.8694(5)	6.1(4)
C(33)	1.0928(7)	0.4810(3)	0.7979(5)	5.7(4)
C(34)	1.0306(7)	0.5757(3)	0.8666(4)	5.3(4)
C(35)	0.9784(6)	0.6223(3)	0.5148(4)	2.9(3)
C(36)	0.8992(9)	0.6767(4)	0.4755(6)	7.3(5)
C(37)	0.9972(8)	0.5793(3)	0.4415(5)	6.5(4)
C(38)	1.1227(8)	0.6438(4)	0.5547(5)	7.9(5)

of the carrying carbon atom). In **2**, hydrogen atoms were treated in a similar way, except for that associated with C(1), which was located from a difference map and not refined. Moreover, in **2**, cavities between the $\text{C}_{46}\text{H}_{50}$ molecules were found to be partially occupied by solvent (CH_2Cl_2 and H_2O). The carbon of CH_2Cl_2 , C(24), was placed at the center of the cavity (site 2*b*) with occupancy 0.125 and two chlorine atoms in site 8*g*, also with occupancy 0.125. One oxygen atom was located in an 8*g* site, and was refined with occupancy 0.25. The stoichiometry was thus fixed to comply with the approximate ratio shown by the NMR spectrum, no attempt being made to refine occupation factors for the disordered atoms. C(24), Cl(1), Cl(2) and O(1) were refined with isotropic temperature factors, and hydrogen atoms associated with the solvent molecules were not included as separate contributions. Thus the CH_2Cl_2 molecule can be visualized as having at least two distinct disordered orientations with respect to the four-fold inversion axis, with 'Cl' representing both Cl

Table 3. Positional and equivalent isotropic thermal parameters, B_{eq} (in Å²), for the non-hydrogen atoms in $\text{C}_{46}\text{H}_{56} \cdot 0.25\text{CH}_2\text{Cl}_2 \cdot 0.5\text{H}_2\text{O}$ (**2**).

Atom	x	y	z	B_{eq}
C(1)	0.7055(4)	0.7426(5)	0.5293(4)	3.7(4)
C(2)	0.6486(5)	0.7241(4)	0.5943(4)	3.0(4)
C(3)	0.5608(5)	0.7628(4)	0.5991(4)	3.5(4)
C(4)	0.5058(4)	0.7450(4)	0.6588(4)	3.4(4)
C(5)	0.5332(4)	0.6876(4)	0.7150(4)	2.9(3)
C(6)	0.6198(4)	0.6492(4)	0.7102(4)	3.1(3)
C(7)	0.6743(4)	0.6670(4)	0.6514(4)	2.9(3)
C(8)	0.4736(4)	0.6700(5)	0.7781(4)	3.6(4)
C(9)	0.4598(4)	0.5951(5)	0.8162(4)	3.6(4)
C(10)	0.4920(4)	0.5014(4)	0.8015(4)	2.8(3)
C(11)	0.5041(4)	0.4703(4)	0.7294(4)	3.0(3)
C(12)	0.5334(4)	0.3838(4)	0.7155(4)	2.7(3)
C(13)	0.5507(4)	0.3291(4)	0.7761(4)	3.2(4)
C(14)	0.5391(4)	0.3557(4)	0.8848(4)	3.0(3)
C(15)	0.5089(4)	0.4438(5)	0.8598(4)	3.0(4)
C(16)	0.5443(4)	0.3468(5)	0.6365(4)	3.4(4)
C(17)	0.6411(5)	0.3118(5)	0.6248(4)	5.0(4)
C(18)	0.5219(7)	0.4140(6)	0.5781(4)	7.7(6)
C(19)	0.4803(5)	0.2651(5)	0.6261(5)	5.8(5)
C(20)	0.5571(5)	0.2935(5)	0.9154(4)	3.9(4)
C(21)	0.6243(7)	0.3360(6)	0.9685(5)	7.7(6)
C(22)	0.5984(7)	0.2048(6)	0.8935(5)	7.9(6)
C(23)	0.4712(7)	0.2768(9)	0.9559(7)	14(1)
C(24)	0.2500	0.2500	0.7500	9(1)
Cl(1)	0.259(1)	0.327(1)	0.695(1)	4.9(6)
Cl(2)	0.200(2)	0.308(2)	0.714(2)	7.8(7)
O(1)	0.265(2)	0.194(2)	0.684(2)	3.9(6)

and H. Partial occupation of a cavity by two water molecules affords an O...O distance of 2.67(5) Å, providing a chemically reasonable model. No attempt was made to resolve the disorder associated with the cavities in more detail. (The cavity is indicated in Fig. 3.)

Further details concerning the refinement of **1** and **2** are given in Table 1. Fractional coordinates and equivalent isotropic thermal parameters for the non-hydrogen atoms in **1** and **2** are given in Tables 2 and 3, and selected bond distances and angles in Tables 4 and 5, respectively. The crystallographic numbering is as in Fig. 1 and 2. A stereo-view of the unit cell of **2** is shown in Fig. 3. Hydrogen-atom coordinates and anisotropic thermal parameters for the non-hydrogen atoms for both structures may be obtained from the authors. Atomic scattering factors and anomalous dispersion corrections were taken from Ref. 5; all calculations were performed using the TEXSAN⁶ software package. Structural illustrations were drawn with ORTEP.⁷

Molecular mechanics calculation

The molecular mechanics (MM) calculations were carried out by a standard molecular mechanics program (Allinger MMP1) on the three conformers in Scheme 1 which all represent local minima on the energy surface. Conformer **2c** has the lowest energy, conformer **2a** 0.2 kcal mol⁻¹ higher and conformer **2b** 0.6 kcal mol⁻¹ higher than **2c**. The differences are too small to be significant, but interestingly

Table 4. Bond distances (in Å) and angles (in °) involving the non-hydrogen atoms in C₃₈H₅₀ (**1**).

C(1)–C(4)	1.408(9)	C(20)–C(21)	1.398(7)
C(2)–C(4)	1.413(10)	C(21)–C(22)	1.378(7)
C(3)–C(4)	1.599(14)	C(22)–C(17)	1.396(7)
C(4)–C(5)	1.528(8)	C(20)–C(23)	1.466(8)
C(5)–C(6)	1.388(7)	C(23)–C(24)	1.334(7)
C(6)–C(7)	1.385(7)	C(24)–C(25)	1.475(7)
C(7)–C(8)	1.400(7)	C(25)–C(26)	1.392(7)
C(8)–C(9)	1.383(7)	C(26)–C(27)	1.396(7)
C(9)–C(10)	1.411(7)	C(27)–C(28)	1.390(7)
C(10)–C(5)	1.400(7)	C(28)–C(29)	1.396(7)
C(9)–C(11)	1.525(7)	C(29)–C(30)	1.396(7)
C(11)–C(12)	1.530(8)	C(30)–C(25)	1.391(7)
C(11)–C(13)	1.537(8)	C(29)–C(31)	1.530(7)
C(11)–C(14)	1.515(8)	C(31)–C(32)	1.518(9)
C(15)–C(7)	1.477(7)	C(31)–C(33)	1.520(8)
C(15)–C(16)	1.331(7)	C(31)–C(34)	1.516(8)
C(16)–C(17)	1.481(8)	C(27)–C(35)	1.535(7)
C(17)–C(18)	1.400(7)	C(35)–C(36)	1.516(9)
C(18)–C(19)	1.372(8)	C(35)–C(37)	1.506(9)
C(19)–C(20)	1.384(7)	C(35)–C(38)	1.523(9)
C(1)–C(4)–C(2)	120.5(8)	C(19)–C(20)–C(21)	116.7(5)
C(1)–C(4)–C(3)	100.0(8)	C(19)–C(20)–C(23)	119.4(5)
C(1)–C(4)–C(5)	114.0(5)	C(21)–C(20)–C(23)	123.8(5)
C(2)–C(4)–C(3)	95.3(9)	C(20)–C(21)–C(22)	121.3(5)
C(2)–C(4)–C(5)	116.2(6)	C(21)–C(22)–C(17)	121.7(5)
C(3)–C(4)–C(5)	105.7(6)	C(20)–C(23)–C(24)	130.1(5)
C(4)–C(5)–C(6)	121.1(5)	C(23)–C(24)–C(25)	128.3(5)
C(4)–C(5)–C(10)	121.2(5)	C(24)–C(25)–C(26)	119.8(5)
C(6)–C(5)–C(10)	117.5(5)	C(24)–C(25)–C(30)	121.2(5)
C(5)–C(6)–C(7)	122.2(5)	C(26)–C(25)–C(30)	119.0(5)
C(6)–C(7)–C(8)	118.3(5)	C(25)–C(26)–C(27)	121.3(5)
C(6)–C(7)–C(15)	120.2(5)	C(26)–C(27)–C(28)	117.8(5)
C(8)–C(7)–C(15)	121.2(5)	C(26)–C(27)–C(35)	120.3(5)
C(7)–C(8)–C(9)	122.3(5)	C(28)–C(27)–C(35)	121.9(5)
C(8)–C(9)–C(10)	117.3(5)	C(27)–C(28)–C(29)	122.8(5)
C(8)–C(9)–C(11)	119.1(5)	C(28)–C(29)–C(30)	117.4(5)
C(10)–C(9)–C(11)	123.5(5)	C(28)–C(29)–C(31)	120.6(5)
C(9)–C(10)–C(5)	122.2(5)	C(30)–C(29)–C(31)	122.0(5)
C(9)–C(10)–C(11)	112.8(5)	C(25)–C(30)–C(29)	121.7(5)
C(9)–C(11)–C(13)	107.4(5)	C(29)–C(31)–C(32)	112.8(5)
C(9)–C(11)–C(14)	110.5(5)	C(29)–C(31)–C(33)	109.8(5)
C(12)–C(11)–C(13)	108.7(5)	C(29)–C(31)–C(34)	109.8(5)
C(12)–C(11)–C(14)	108.2(5)	C(32)–C(31)–C(33)	108.5(5)
C(13)–C(11)–C(14)	109.0(5)	C(32)–C(31)–C(34)	107.0(5)
C(7)–C(15)–C(16)	128.8(5)	C(33)–C(31)–C(34)	108.8(5)
C(15)–C(16)–C(17)	130.3(5)	C(27)–C(35)–C(36)	110.7(5)
C(16)–C(17)–C(18)	119.1(5)	C(27)–C(35)–C(37)	109.7(5)
C(16)–C(17)–C(22)	124.0(5)	C(27)–C(35)–C(38)	113.0(5)
C(18)–C(17)–C(22)	116.8(5)	C(36)–C(35)–C(37)	108.7(6)
C(17)–C(18)–C(19)	121.0(5)	C(36)–C(35)–C(38)	107.0(6)
C(18)–C(19)–C(20)	122.5(5)	C(37)–C(35)–C(38)	107.7(6)

enough, the MM calculations result in a lowest energy for the helical conformer that is almost identical to that in the crystal.

Discussion

In both compounds **1** and **2** a helical arrangement of the backbone chain is preferred in the solid state. This is also the best conformation based on molecular mechanics calculations on unsubstituted bis(styryl)stilbene. For compari-

Table 5. Bond distances (in Å) and angles (in °) involving the non-hydrogen atoms in the C₄₆H₅₆ molecule in **2**.^a

C(1)–C(1')	1.334(13)	C(12)–C(13)	1.382(8)
C(1)–C(2)	1.467(9)	C(13)–C(14)	1.378(8)
C(2)–C(3)	1.422(9)	C(14)–C(15)	1.392(8)
C(3)–C(4)	1.373(9)	C(15)–C(16)	1.374(8)
C(4)–C(5)	1.382(9)	C(12)–C(16)	1.532(9)
C(5)–C(6)	1.404(8)	C(16)–C(17)	1.537(9)
C(6)–C(7)	1.357(9)	C(16)–C(18)	1.484(10)
C(7)–C(2)	1.384(9)	C(16)–C(19)	1.546(9)
C(5)–C(8)	1.461(9)	C(14)–C(20)	1.533(9)
C(8)–C(9)	1.319(9)	C(20)–C(21)	1.516(10)
C(9)–C(10)	1.489(9)	C(20)–C(22)	1.501(10)
C(10)–C(11)	1.388(8)	C(20)–C(23)	1.484(11)
C(11)–C(12)	1.373(8)		
C(i)–C(1)–C(2)	126.6(4)	C(13)–C(12)–C(16)	120.2(6)
C(1)–C(2)–C(3)	119.9(6)	C(12)–C(13)–C(14)	124.0(6)
C(1)–C(2)–C(7)	123.3(7)	C(13)–C(14)–C(15)	116.3(6)
C(3)–C(2)–C(7)	116.8(7)	C(13)–C(14)–C(20)	123.3(6)
C(2)–C(3)–C(4)	120.8(6)	C(15)–C(14)–C(20)	120.4(6)
C(3)–C(4)–C(5)	121.1(7)	C(14)–C(15)–C(16)	122.0(6)
C(4)–C(5)–C(6)	118.1(7)	C(12)–C(16)–C(17)	110.2(6)
C(4)–C(5)–C(8)	120.1(6)	C(12)–C(16)–C(18)	113.2(6)
C(6)–C(5)–C(8)	121.8(7)	C(12)–C(16)–C(19)	109.1(6)
C(5)–C(6)–C(7)	120.8(7)	C(17)–C(16)–C(18)	109.6(7)
C(6)–C(7)–C(2)	122.3(6)	C(17)–C(16)–C(19)	106.9(6)
C(5)–C(8)–C(9)	130.3(7)	C(18)–C(16)–C(19)	107.6(7)
C(8)–C(9)–C(10)	129.7(7)	C(14)–C(20)–C(21)	111.0(6)
C(9)–C(10)–C(11)	121.1(6)	C(14)–C(20)–C(22)	112.9(7)
C(9)–C(10)–C(15)	119.9(6)	C(14)–C(20)–C(23)	109.5(7)
C(11)–C(10)–C(15)	119.0(6)	C(21)–C(20)–C(22)	105.1(7)
C(10)–C(11)–C(12)	121.3(6)	C(21)–C(20)–C(23)	108.7(9)
C(11)–C(12)–C(13)	117.4(6)	C(22)–C(20)–C(23)	109.4(8)
C(11)–C(12)–C(16)	122.3(6)		

^aSymmetry code (i): 1.5–x, 1.5–y, z.

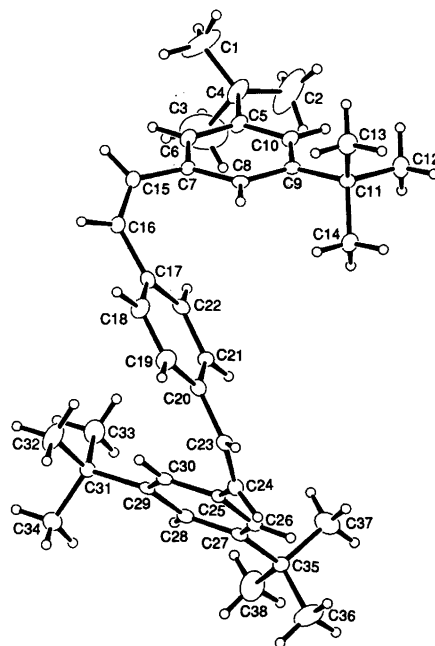


Fig. 1. Molecular structure of a bis(styryl)benzene (**1**) showing the crystallographic numbering. Thermal ellipsoids enclose 50% probability.

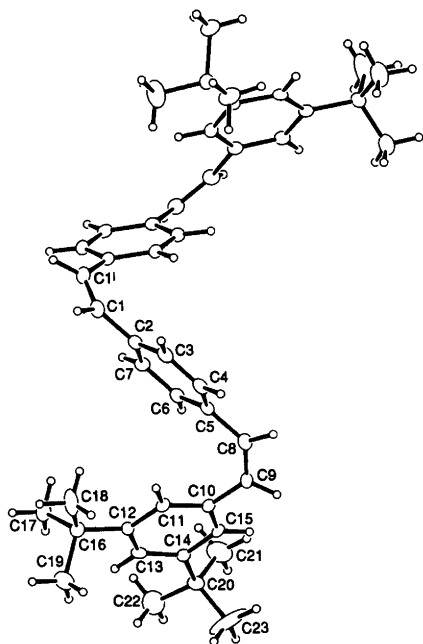


Fig. 2. Molecular structure of a bis(styryl)stilbene (**2**) showing the crystallographic numbering. Thermal ellipsoids enclose 50% probability. For symmetry code see Table 5.

son the X-ray and calculated structures are shown in Fig. 4 to a best fit omitting the *tert*-butyl groups in the X-ray structure for clarity. The structures overlap closely with a slightly wider helix for the X-ray structure which has four *tert*-butyl substituents. These are omitted in the calculated structure. It is clear that the effect of the substituents on the structure is small, and it seems reasonable to assume that the same conclusion is also valid for the photochemical reaction mechanism.

From a photochemical point of view, the overlap in the extended π -system is important in order to rationalise the adiabatic mechanism which has been observed for the triplet-state reaction of **1** and singlet-state reaction of **1** and **2**.^{2,9} The relative energies of the 'planar' and 'twisted' excited states determine the reaction path and mechanism for the *Z/E* photoisomerization. The dihedral angles for the

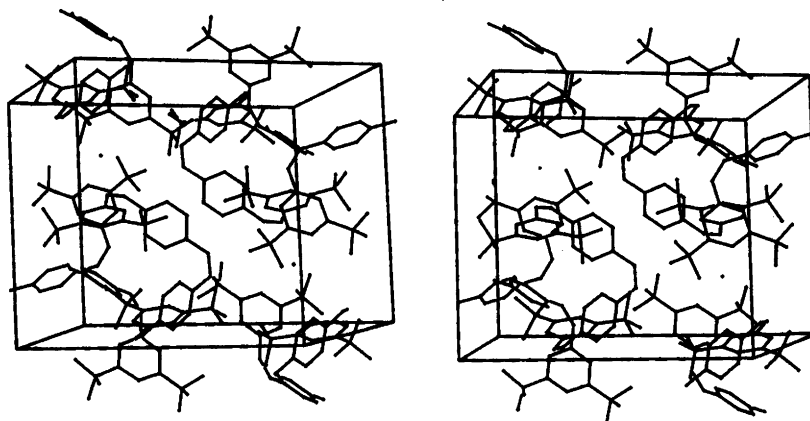


Fig. 3. Stereoview of the unit cell of **2** with the cavities marked as dots. The *c* axis is horizontal.

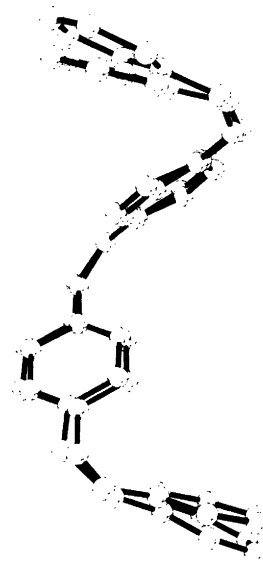


Fig. 4. A comparison between the calculated structure of 4,4'-bis(styryl)stilbene, wider helix (Allingers MMP2 force field) and the crystal structure of 4,4'-bis(3,5-di-*tert*-butyl)stilbene. The *tert*-butyl groups have been omitted for clarity.

bonds between the benzene rings and the vinylene groups (shown in Figs. 1 and 2) vary between 31.8 and 40.8°. In stilbene the angle has been determined (for *cis*-stilbene) to be ca. 43° (C_2 symmetry) by electron diffraction methods in the gas phase.¹⁰

Acknowledgements. Financial support from the Swedish Natural Science Research Council and the Swedish Board of Technical Development is gratefully acknowledged.

References

1. Saltiel, J. and Charlton, J. L. In: de Mayo, P., Ed., *Rearrangement in Ground and Excited States*, Academic Press, New York 1980, Vol. 3.
2. Sandros, K., Sundahl, M., Wennerström, O. and Norinder, U. *J. Am. Chem. Soc.* **112** (1990) 3082.
3. Wennerström, O., Raston, I., Sundahl, M. and Tanner, D. *Chem. Scr.* **27** (1987) 567.

4. Gilmore, C. J. *J. Appl. Crystallogr.* 17 (1984) 42.
5. *International Tables for X-ray Crystallography*, Kynoch Press, Birmingham 1974, Vol. IV.
6. *TEXSAN-TEXRAY Structure Analysis Package*, Molecular Structure Corporation, Texas 1989.
7. Johnson, C. K. *ORTEP: Report ORNL-3794*, Oak Ridge National Laboratory, Oak Ridge, TN 1965.
8. Burkert, U. and Allinger, N. L. *ACS Monogr 177*, American Chemical Society, Washington, DC 1982.
9. Sundahl, M., Wennerström, O., Sandros, K., Arai, T. and Tokumaru, K. *J. Phys. Chem.* 94 (1990) 6731.
10. Traetteberg, M. and Frantsen, A. *J. Mol. Struct.* 26 (1975) 69.

Received April 13, 1992.